equilibration of the cage with mononuclear species. Unsymmetrical cages of nuclearity 3 and 4 that provide inequivalent, bridged $M^{II}(SR)_4$ sites with tetrahedral stereochemistry are a requisite step toward the simulation of the M(II) site aggregates in metallothionein.

Acknowledgment. This research was supported by NIH Grant GM 28856. NMR and X-ray diffraction equipment used in this research were obtained by NSF Grants CHE 80-00670 and CHE 80-08891. We thank J. M. Berg for the volume calculations in Table IV and Professor D. Coucouvanis for a preprint of ref 19.

Registry No. $(Me_4N)_2[Zn_2(SPh)_{10}]$, 76915-21-4; $(Et_4N)_2[Zn_4(SPh)_{10}]$, 82665-17-6; $(Et_4N)_2[Cd(SPh)_4]$, 82665-18-7; $(Me_4N)_2[Fe_4(SPh)_{10}]$, 74829-06-4; $[Fe_4(SPh)_{10}]^{2-}$, 74829-05-3; $[Co_4(SPh)_{10}]^{2-}$, 57659-25-3; $[Zn_4(SPh)_{10}]^{2-}$, 76915-20-3; $[Cd_4(SPh)_{10}]^{2-}$, 82665-19-8; $(Et_4N)_2[Cd_4(SPh)_{10}]$, 82665-20-1.

Supplementary Material Available: Crystal structure data for $(Me_4N)_2[Fe_4(SPh)_{10}]\cdot C_4H_7N$ including thermal parameters of the anion (Table S-I), positional and thermal parameters of the cations and solvate molecule (Table S-II), calculated H atom coordinates (Table S-III), and calculated and observed structure factors (Table S-IV) (39 pages). Ordering information is given on any current masthead page.

Contribution from the Institut für Anorganische Chemie and the Laboratorium für Kristallographie, Universität Bern, CH-3000 Bern 9, Switzerland

Syntheses and Crystal and Molecular Structures of Hexaaquaruthenium(II) *p*-Toluenesulfonate and Hexaaquaruthenium(III) *p*-Toluenesulfonate, $[Ru(H_2O)_6](C_7H_7SO_3)_2$ and $[Ru(H_2O)_6](C_7H_7SO_3)_3\cdot 3H_2O$

PAUL BERNHARD,[1a] HANS-BEAT BÜRGI,*[1b] JÜRG HAUSER,[1b] HANS LEHMANN,[1a] and ANDREAS LUDI*[1a]

Received March 22, 1982

Crystals of $Ru(H_2O)_6(tos)_2$ (II) (tos^- is *p*-toluenesulfonate) were grown from aqueous $Ru(H_2O)_6^{2+}$ solutions obtained by reduction of RuO_4 solutions with metallic lead. Crystals of $Ru(H_2O)_6(tos)_3\cdot 3H_2O$ (III) were grown from aqueous $Ru(H_2O)_6^{3+}$ obtained by oxidation of a $Ru(H_2O)_6^{2+}$ solution with O_2. For II the space group is $P\bar{1}$ with cell parameters a = 6.138 (1) Å, b = 7.287 (2) Å, c = 12.423 (4) Å, α = 92.22 (2)°, β = 94.82 (2)°, γ = 107.13 (2)°, and Z = 1. For III the space group is $C2/c$ with lattice constants a = 25.466 (7) Å, b = 7.235 (4) Å, c = 35.113 (8) Å, β = 93.97 (2)°, and Z = 8. The structure of II was refined to R = 3.3% for 2302 reflections with $F_o > \sigma(F_o)$; the structure of III, to R = 5.2% for 2989 reflections with $F_o > \sigma(F_o)$. In both structures $Ru(H_2O)_6$ octahedra are linked by hydrogen bonds to the SO_3 groups of the anion, the O-H···O distances ranging from ~2.5 to 3.0 Å. The average metal–oxygen distance is 2.122 (16) Å for Ru(II)–OH_2 and 2.029 (7) Å for Ru(III)–OH_2. The effect of the change in bond length on the rate of the $Ru(H_2O)_6^{3+/2+}$ self-exchange reaction is discussed.

Introduction

The coordination chemistry of ruthenium in oxidation states II and III is dominated by nitrogen donors.[2] The preparative chemistry as well as thermodynamic and kinetic properties for a broad range of ammine complexes has been thoroughly studied by Taube and his co-workers.[3] Many of these studies have been concerned with electron-transfer reactions, including self-exchange reactions. The comparison of these results with the behavior of first-row transition elements and the relationship between the electron-transfer kinetics and structural parameters continue to pose intriguing and sometimes puzzling problems.[4] In contrast to the wealth of information available for the ruthenium ammines, surprisingly few studies have dealt with the hexaaqua ions of ruthenium,[5-9] with most investigations confined to dilute solutions. The case of the ruthenium aqua ions deserves special attention since the pair $Ru(H_2O)_6^{3+}/Ru(H_2O)_6^{2+}$ is so far the only example of a low-spin t_{2g}^5–t_{2g}^6 redox couple within the metal aqua ions. Of prime interest, again, are the self-exchange reaction and the connection of the corresponding kinetic parameters to the molecular structure. The application of the Marcus cross relation to a series of redox reactions involving either $Ru(H_2O)_6^{3+}$ or $Ru(H_2O)_6^{2+}$ led to an estimate of 60 ± 40 M^{-1} s^{-1} for the rate constant of the self-exchange reaction. Sutin concluded from these data that there exists a difference of approximately 0.1 Å between the ruthenium–oxygen bond lengths in the two aqua ions.[8] We therefore focused our efforts on isolating and investigating crystalline salts of $Ru(H_2O)_6^{3+}$ and $Ru(H_2O)_6^{2+}$. A special bonus of these efforts resulted for the preparative inorganic chemist: the availability of a stable solid salt of $Ru(H_2O)_3^{2+}$ as a starting material opens up new and facile synthetic routes to a variety of ruthenium complexes.[10]

Experimental Section

A. Preparations. $Ru(H_2O)_6^{2+}$. The $Ru(H_2O)_6^{2+}$ solutions prepared according to Kallen and Earley[7] contained substantial amounts of tin, as was shown by atomic absorption spectroscopy. We therefore used a different synthetic procedure: A 1.5-g sample of Ru metal was fused in a Ni crucible with 30 g of KOH. A 3-g amount of

(1) (a) Institut für Anorganische Chemie. (b) Laboratorium für Kristallographie.
(2) Cotton, F. A.; Wilkinson, G. "Advanced Inorganic Chemistry", 4th ed.; Interscience: New York, 1980; Chapter 22-F.
(3) Taube, H. *Comments Inorg. Chem.* **1981**, *1*, 17.
(4) Sutin, N. *Tunneling Biol. Syst. [Proc. Symp.] 1977* **1979**, 201.
(5) Cady, H. H.; Connick, R. E. *J. Am. Chem. Soc.* **1958**, *80*, 2646.
(6) Mercer, E. E.; Buckley, R. R. *Inorg. Chem.* **1965**, *4*, 1692.
(7) Kallen, T. W.; Earley, J. E. *Inorg. Chem.* **1971**, *10*, 1149.
(8) Böttcher, W.; Brown, G. M.; Sutin, N. *Inorg. Chem.* **1979**, *18*, 1447.
(9) Harzion, Z.; Navon, G. *Inorg. Chem.* **1980**, *19*, 2236.
(10) Bernhard, P.; Lehmann, H.; Ludi, A. *J. Chem. Soc., Chem. Commun.* **1981**, 1216.

0020-1669/82/1321-3936$01.25/0

Table I. Crystal Data for $Ru(H_2O)_6(tos)_2$ (II) and $Ru(H_2O)_6(tos)_3 \cdot 3H_2O$ (III)

	II	III
space group	$P\bar{1}$	$C2/c$
a, Å	6.138 (1)	25.466 (7)
b, Å	7.287 (2)	7.235 (4)
c, Å	12.423 (4)	35.113 (8)
α, deg	92.22 (2)	
β, deg	94.82 (2)	93.97 (2)
γ, deg	107.13 (2)	
V, Å^3	527.8	6453.9
fw	551.4	776.8
Z	1	8
D_{measd}(flotation), g cm^{-3}	1.73 (1)	1.61 (1)
D_{calcd}, g cm^{-3}	1.735	1.599

Table II. Intensity Collection and Refinement for II and III

	II	III
cryst dimens, mm	0.18 × 0.2 × 0.21	0.07 × 0.16 × 0.09
linear abs coeff, cm^{-1}	9.8	7.4
2θ limits, deg	1-56	1-46
scan width, deg	0.8 + 0.35 tan θ	0.7 + 0.35 tan θ
no. of unique refl measd	2665	4479
no. of unique refl with $F_o > \sigma(F_o)$	2302	2989
no. of parameters	133	435
R, %	3.3	5.2
R_w, %	4.4	5.3
goodness of fit	1.96	2.01
final shift/error	<0.01	<0.01

$KMnO_4$ was added in small portions, and the mixture was heated to red glow for 1 h. After cooling, the solidified melt was dissolved in 250 mL of water in a 1-L flask connected to a condenser and a series of three traps. All the joints were absolutely grease free. A 1.5-g amount of $KMnO_4$ and 200 mL of H_2SO_4 (50%) were added to the flask. RuO_4 evolved and was swept by a stream of O_2 through the condenser into the ice-cooled traps containing altogether 350 mL of 1 M H_2SiF_6. The last parts of RuO_4 were gained by boiling the reaction mixture. Owing to the toxicity of RuO_4 the operation had to be carried out in a well-ventilated hood. The combined contents of the traps were reduced overnight in a 1-L Schlenk vessel with 30 g of activated Pb (15 min in 30% HNO_3). To the filtered pink solution was added 40 g of $Na_2SO_4 \cdot 10H_2O$. After 0.5 h solid $PbSO_4$ was removed by filtration through a G3 frit and then through a 0.22-μm Millipore filter. The filtrate was diluted to 1050 mL and loaded onto an ion-exchange column (35 g of Dowex 50W in the H^+ form). $Ru(H_2O)_6^{2+}$ was eluted with 1 M Htos (tos^- = *p*-toluenesulfonate). The resulting solution contained less than 10 ppm of Pb. Concentration in a rotating evaporator under reduced pressure at 35 °C to ca. 120 mL produced a precipitate of $Ru(H_2O)_6(tos)_2$ (II). Heating to 40–50 °C redissolved the solid. Slow cooling to −2 °C gave pink, irregularly prismatic crystals which were isolated by filtration, washed with ethyl acetate, and dried under vacuum. Reduction, ion exchange, and crystallization were carried out under argon. Yield: 50–60%. Anal. Calcd for $Ru(H_2O)_6(tos)_2$ (II): Ru, 18.33; C, 30.49; H, 4.75; S, 11.63; H_2O, 19.6. Found: Ru, 18.6; C, 30.8; H, 4.7; S, 11.5; H_2O, 19.1; Pb contamination in the solid <0.5 ppm.

$Ru(H_2O)_6^{3+}$. The solution of II obtained by ion exchange was concentrated to 250 mL and oxidized with O_2 for 3–5 h to produce a yellow solution. Precipitation, redissolution, and crystallization as for II produced lemon-colored needle-shaped crystals. Yield: 30–40% referred to Ru metal. Anal. Calcd for $Ru(H_2O)_6(tos)_3 \cdot 3H_2O$ (III): Ru, 13.01; C, 32.47; H, 5.06; S, 12.38; H_2O, 20.85. Found: Ru, 13.4; C, 32.6; H, 5.1; S, 12.3; Pb, <0.1 ppm.

The crystals of II and III were perfectly air stable for a period of several months in surprising contrast to the aqueous solution of II, which was easily oxidized by aerial oxygen.

Various attempts were made to isolate salts of other inert anions. Crystals were also obtained with the anion trifluoromethanesulfonate; the salt of $Ru(H_2O)_6^{3+}$, however, was extremely hygroscopic. The standard inert anion ClO_4^- was quantitatively reduced by $Ru(H_2O)_6^{2+}$. The concentration of free F^- in acidic solutions of SiF_6^{2-} and PF_6^- was sufficient to produce mixed fluoro–aqua complexes. The pink crystals of $Ru(H_2O)_6(BF_4)_2$ deteriorated at room temperature within a few days under liberation of HF.

Ru was analyzed spectrophotometrically.[11] The elemental analyses were performed by Ciba-Geigy, Basel.

Table III. Final Atomic Positional Parameters and B_{eq} Values, with Standard Deviations in Parentheses, for II[a]

atom	x/a	y/b	z/c	B_{eq}, Å^2
Ru	0.0000 (0)	0.0000 (0)	0.0000 (0)	1.94 (2)
S	0.2749 (1)	0.5934 (1)	0.20235 (6)	2.24 (4)
O1	0.2173 (4)	−0.1594 (3)	−0.0537 (2)	2.65 (8)
O2	0.2084 (4)	0.2524 (3)	−0.0593 (2)	3.14 (9)
O3	0.2061 (4)	0.0735 (3)	0.1503 (2)	3.03 (9)
O4	0.0419 (4)	0.5152 (3)	0.1499 (2)	2.79 (8)
O5	0.4004 (4)	0.7684 (3)	0.1528 (2)	2.67 (8)
O6	0.4038 (4)	0.4562 (3)	0.2083 (2)	3.25 (10)
C1	0.2501 (6)	0.6660 (5)	0.3369 (3)	2.46 (7)
C2	0.0611 (7)	0.7109 (7)	0.3646 (4)	4.8 (3)
C3	0.0496 (7)	0.7692 (8)	0.4700 (4)	5.3 (3)
C4	0.2225 (7)	0.7826 (6)	0.5503 (3)	3.5 (2)
C5	0.4131 (8)	0.7408 (8)	0.5209 (4)	4.8 (3)
C6	0.4258 (7)	0.6781 (7)	0.4149 (4)	4.5 (2)
C7	0.2069 (9)	0.8426 (7)	0.6668 (4)	5.2 (3)

[a] $B_{eq} = {}^4/_3 \Sigma_i \Sigma_j B_{ij} a_i \cdot a_j$ (a_i, a_j: crystal axes). Numbering scheme: O1, O2, O3, coordinated water molecules; O4, O5, O6, SO_3 group; C1–C6, ring atoms; C7, methyl carbon.

B. Collection and Reduction of Diffraction Data. Lattice constants (Table I) and intensities of II and III were measured at 22 °C on a CAD-4 diffractometer using Mo Kα radiation (graphite monochromator, λ = 0.71069 Å). Cell parameters were determined by least-squares optimization of 14 accurately centered reflections in the θ range between 10 and 17.5°. Details of data collection and refinement process are summarized in Table II. For both crystals the three check reflections recorded every 150 min did not show systematic intensity fluctuations. The intensities were corrected for Lorentz–polarization effects but not for absorption. Neutral-atom scattering factors were chosen[12] with anomalous dispersion corrections for Ru and S.[13] All calculations were performed on a PDP 11/34 by using versions 17 and 18 of the structure determination package of Enraf-Nonius (SDP). ORTEP drawings were made on a IBM 3033 computer with the XRAY 76 program system.

C. Solution and Refinement of the Structures. Since the primary aim of our study is the direct comparison of the geometries of $Ru(H_2O)_6^{3+}$ and $Ru(H_2O)_6^{2+}$, we carefully followed the same pattern in reducing and refining the data for both structures II and III. The structure of II with one formula unit in the cell of space group $P\bar{1}$ was solved by Patterson and Fourier methods. In the case of III the Patterson synthesis revealed two structurally inequivalent sites for the ruthenium atoms: one, at position 4a (0, 0, 0; 0, 0, $^1/_2$), has site symmetry $\bar{1}$; the other, 4e (0, y, $^1/_4$; 0, $\bar{y}$, $^3/_4$), site symmetry 2. Unexpectedly large thermal parameters were obtained for the oxygen atoms of the $Ru(H_2O)_6^{3+}$ unit at position 4a. Close inspection of a Fourier map showed resolved peaks of equal heights for two of the three symmetry-independent O atoms. Splitting these oxygens (O2 and O3) into two sets with equal occupation (Figure 3) led to a significant improvement in the model. The disorder implied in the orientation of this $Ru(H_2O)_6^{3+}$ octahedron can be described roughly as a torsion by ca. 27° around an axis nearly coinciding with O1···Ru···O1′ (Figures 3 and 4). The unresolved O atom O1 has relatively high thermal parameters perpendicular to the Ru–O vector (Figure 4). The two different orientations of this hexaaqua unit are matched by a corresponding disorder of the SO_3 groups (O23 and O33) connected to the coordinated water molecules by hydrogen bonds.

Hydrogen atoms of the phenyl rings were included in the structure factor calculations during the last stages of the refinement. A fixed C–H bond length of 0.96 Å and an isotropic temperature factor of 5.0 Å^2 were chosen. It was not possible to locate the H atoms of the water molecules and of the methyl groups: a ΔF map showed chemically insignificant residual electron density peaks smaller than

(11) Marshall, E. D.; Rickard, R. R. *Anal. Chem.* **1950**, *22*, 795. Woodhead, J. L.; Fletcher, J. M. *J. Chem. Soc.* **1961**, 5039.
(12) Cromer, D. T.; Waber, J. T. "International Tables for X-Ray Crystallography"; Kynoch Press: Birmingham, England, 1974; Vol. IV, Table 2.2B.
(13) Cromer, D. T. Reference 12, Table 2.3.1.

Table IV. Final Atomic Positional Parameters and B_{eq} Values, with Standard Deviations in Parentheses, for III[a]

atom	x/a	y/b	z/c	B_{eq}, Å^2
Ru1	0.0000 (0)	0.0000 (0)	0.0000 (0)	2.41 (7)
Ru2	0.0000 (0)	0.4746 (1)	0.2500 (0)	2.44 (7)
S1	0.09440 (7)	−0.0255 (2)	0.20643 (5)	3.1 (2)
S2	−0.1048 (1)	−0.5524 (5)	0.06763 (7)	8.9 (2)
S3	0.0774 (1)	0.5457 (5)	0.09379 (7)	7.6 (1)
O1	0.0489 (2)	−0.2182 (8)	0.0074 (2)	8.0 (5)
O2	0.0518 (4)	0.163 (1)	−0.0259 (2)	3.8 (6)
O2*	0.0457 (4)	0.064 (1)	−0.0431 (3)	4.0 (3)
O3	0.0315 (4)	0.070 (1)	0.0528 (3)	3.7 (5)
O3*	0.0409 (4)	0.171 (1)	0.0368 (3)	4.1 (6)
O4	0.0566 (2)	0.4739 (7)	0.2117 (1)	3.6 (3)
O5	0.0411 (2)	0.2761 (6)	0.2794 (1)	3.6 (3)
O6	−0.0404 (2)	0.6746 (6)	0.2198 (1)	3.2 (2)
O7	0.4728 (2)	0.2513 (9)	0.1490 (1)	5.3 (4)
O8	0.0420 (3)	0.217 (1)	0.3506 (2)	7.9 (5)
O9	−0.0844 (4)	−0.065 (1)	0.0901 (3)	4.7 (6)
O9*	0.0726 (9)	0.059 (2)	0.1024 (4)	11 (1)
O11	0.0786 (2)	−0.0273 (7)	−0.2458 (1)	3.9 (4)
O12	0.0742 (2)	0.1360 (7)	0.1857 (1)	3.8 (4)
O13	0.0816 (2)	−0.1970 (7)	0.1866 (1)	3.8 (4)
O21	−0.1008 (3)	−0.754 (1)	0.0659 (2)	10.5 (5)
O22	−0.0937 (3)	−0.489 (1)	0.1057 (2)	10.3 (5)
O23	−0.0704 (4)	−0.531 (1)	0.0336 (3)	3.8 (4)
O23*	−0.0788 (5)	−0.395 (2)	0.0457 (4)	5.8 (8)
O31	0.0619 (3)	0.739 (1)	0.0923 (2)	9.8 (7)
O32	0.0507 (2)	0.449 (1)	0.1226 (2)	8.0 (6)
O33	0.0720 (4)	0.399 (1)	0.0621 (3)	4.1 (6)
O33*	0.0733 (4)	0.533 (1)	0.0501 (3)	4.0 (6)
C11	0.1639 (3)	−0.006 (1)	0.2098 (2)	3.0 (3)
C12	0.1913 (3)	−0.058 (1)	0.1793 (2)	3.7 (4)
C13	0.2446 (3)	−0.036 (1)	0.1805 (2)	4.6 (5)
C14	0.2725 (3)	0.039 (1)	0.2122 (3)	4.7 (5)
C15	0.2440 (4)	0.089 (1)	0.2424 (2)	4.9 (5)
C16	0.1905 (3)	0.069 (1)	0.2416 (2)	4.1 (4)
C17	0.3321 (4)	0.059 (2)	0.2127 (4)	7.4 (9)
C21	−0.1710 (3)	−0.497 (1)	0.0554 (2)	3.3 (3)
C22	−0.1922 (4)	−0.547 (2)	0.0203 (2)	5.8 (6)
C23	−0.2446 (4)	−0.510 (2)	0.0102 (3)	6.4 (6)
C24	−0.2769 (4)	−0.426 (1)	0.0343 (3)	5.8 (5)
C25	−0.2535 (4)	−0.376 (1)	0.0691 (3)	7.3 (8)
C26	−0.2020 (4)	−0.410 (1)	0.0800 (2)	5.9 (6)
C27	−0.3343 (4)	−0.390 (2)	0.0228 (4)	9.2 (9)
C31	0.1453 (3)	0.541 (1)	0.1078 (2)	4.2 (4)
C32	0.1805 (4)	0.639 (1)	0.0873 (2)	5.3 (5)
C33	0.2336 (4)	0.635 (1)	0.0990 (2)	5.2 (5)
C34	0.2525 (3)	0.539 (1)	0.1302 (2)	4.4 (4)
C35	0.2169 (4)	0.445 (1)	0.1506 (2)	4.6 (4)
C36	0.1638 (3)	0.444 (1)	0.1396 (2)	4.6 (4)
C37	0.3116 (4)	0.537 (2)	0.1422 (3)	6.7 (6)

[a] $B_{eq} = {}^4/_3 \Sigma_i \Sigma_j B_{ij} a_i \cdot a_j$ (a_i, a_j: crystal axes). In this and all subsequent tables and figures of III, O and O* represent the two sets of disordered oxygen positions. Numbering scheme: O1, O2, O3, coordinated water molecules of Ru1; O4, O5, O6, coordinated water molecules of Ru2; *Oi*1–*Oi*3, SO_3 group of atom S*i*; O7, O8, O9, uncoordinated lattice water; C*i*1–C*i*6, ring atoms; C*i*7, methyl carbon.

0.4 e/Å^3. During least-squares refinement the function $\sum w(F_o - F_c)^2$ was minimized with $w = 4F_o^2/[(\sigma(I))^2 + (pI)^2]$, $p = 0.02$ for II and III. The final atomic coordinates are given in Tables III and IV. Tables of the thermal parameters and the hydrogen positions as well as listings of the structure factors are available as supplementary material.

Description and Discussion of the Structures

The crystal structures of both hexaaquaruthenium salts are adequately described as layer structures. Sheets of anions and cations alternate in a regular fashion as illustrated in Figures 1 and 2. The layers are parallel to the *a,b* plane for $Ru(H_2O)_6(tos)_2$ (II) and to the *b,c* plane for $Ru(H_2O)_6(tos)_3 \cdot 3H_2O$ (III). In both structures the phenyl rings of the *p*-toluenesulfonate anions are approximately perpendicular to the layer plane; the SO_3 groups in the structure of II alternate in pointing to the cation sheets above and below the anion layer. The three uncoordinated water molecules in the structure of III are all located within the cation layer (Figure 2). Important packing forces are the hydrogen bonds linking the coordinated water molecules to the SO_3 groups (Table V). The network of the hydrogen bonds extends along the *b* direction for II and in the *b,c* plane for III. If we allow for disorder, the molecular structures of the *p*-toluenesulfonate anions in II and III fit the expected pattern and do not require special comment. Tables with the interatomic distances and least-squares planes are available as supplementary material.

Both structures exhibit the expected octahedral coordination geometry of the hexaaqua ions (Tables VI and VII). The small deviations from ideal octahedral geometry are attributed to effects of the hydrogen bonds, i.e., to the crystal packing. The largest difference within the Ru–O bond lengths of either II or III is 0.03 Å, comparable to the scatter of the metal to

Table V. Hydrogen Bonds between the Hexaaqua Ions and the SO_3 Groups or Lattice Water (O1, O8, O9, O9*) in II and III (<3.0 Å)

	II		
O1-H-O4	2.774 (2)	O2-H-O5	2.794 (3)
O1-H-O5	2.843 (3)	O3-H-O5	2.816 (2)
O2-H-O4	2.808 (2)	O3-H-O6	2.733 (3)
	III		
$O1_c$-H-O21	2.80[a]	O4-H-O12	2.66
$O1_c$-H-O33*	2.52[a]	O4-H-O13	2.63
O2-H-O9	2.56	O5-H-O8	2.53
O2-H-O23	2.72	O5-H-O11	2.70
O3-H-O31	2.85	O6-H-O11	2.69
O3-H-O33	2.61	O6-H-O7	2.59
$O1_c$*-H-O31	2.79[a]	O9-H-O7	2.78
$O1_c$*-H-O23	2.55[a]	O9-H-O21	2.43[b]
O2*-H-O21	2.79	O9*-H-O12	2.98
O2*-H-O23*	2.54	O9*-H-O31	2.36[b]
O3*-H-O9*	2.52	O9*-H-O32	2.97
O3*-H-O33*	2.77	O8-H-O22	2.89
		O7-H-O22	2.80

[a] Estimated positions of $O1_c$ and $O1_c$* (▲ in Figure 4): $O1_c$ (0.0486, −0.221, 0.0016), $O1_c$* (0.0491, −0.215, 0.0132). [b] O21 and O31 show high apparent thermal motion approximately in the direction of these hydrogen bonds. If O21 and O31 were resolved into two (e.g., O21, O21* and O31, O31*, analogous to O1 → $O1_c$, $O1_c$*), the distances O9···O21 and O9*···O31 would increase by about 0.1–0.2 Å. The distances O2*···O21 and O3···O31 would decrease correspondingly (Figure 5).

Table VI. Selected Interatomic Distances (Å) and Angles (Deg) for II

Ru-O1	2.139 (2)	O1-Ru-O2	89.30 (7)
Ru-O2	2.107 (2)	O1-Ru-O3	89.98 (7)
Ru-O3	2.121 (2)	O2-Ru-O3	88.71 (8)
$\langle Ru-O \rangle_{av}$	2.122 (16)		

Table VII. Selected Interatomic Distances (Å) and Angles (Deg) for III

Ru1-O1	2.016 (4)	O1-Ru1-O2	84.37 (14)
Ru1-O2	2.030 (4)	O1-Ru1-O2*	83.94 (14)
Ru1-O2*	2.026 (4)	O1-Ru1-O3	82.89 (17)
Ru1-O3	2.031 (4)	O1-Ru1-O3*	83.66 (21)
Ru1-O3*	2.026 (6)	O2-Ru1-O3	88.02 (17)
		O2*-Ru1-O3*	87.72 (18)
		O2-Ru1-O2*	26.90 (14)
		O3-Ru1-O3*	27.42 (20)
Ru2-O4	2.037 (5)	O4-Ru2-O5	88.29 (22)
Ru2-O5	2.019 (6)	O4-Ru2-O6	89.48 (22)
Ru2-O6	2.031 (7)	O5-Ru2-O6	90.78 (25)
$\langle Ru-O \rangle_{av}$	2.029 (7)[a]		

[a] Ru-O1 is not included in the average because of the disorder (see text).

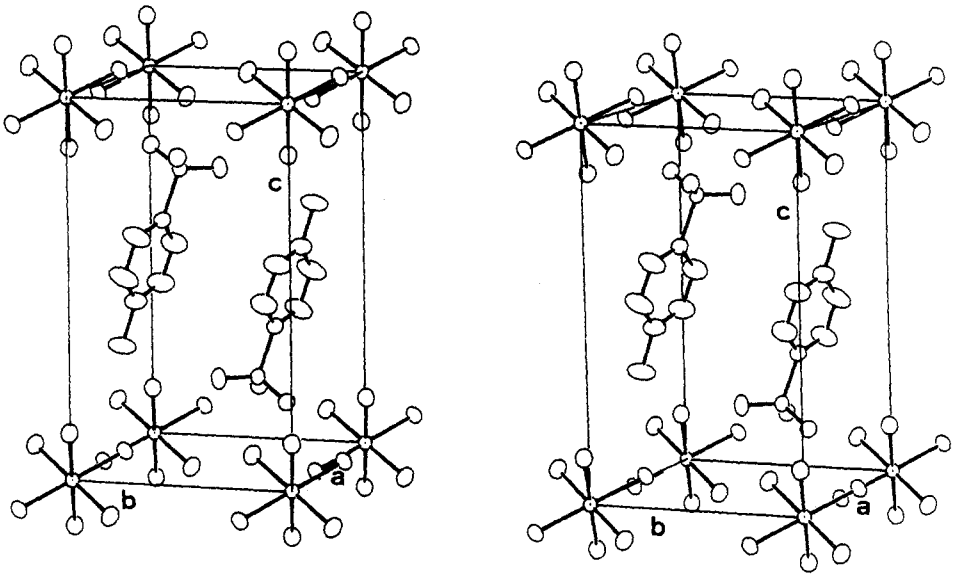

Figure 1. Stereoscopic view of the unit cell of $Ru(H_2O)_6(tos)_2$ (II).

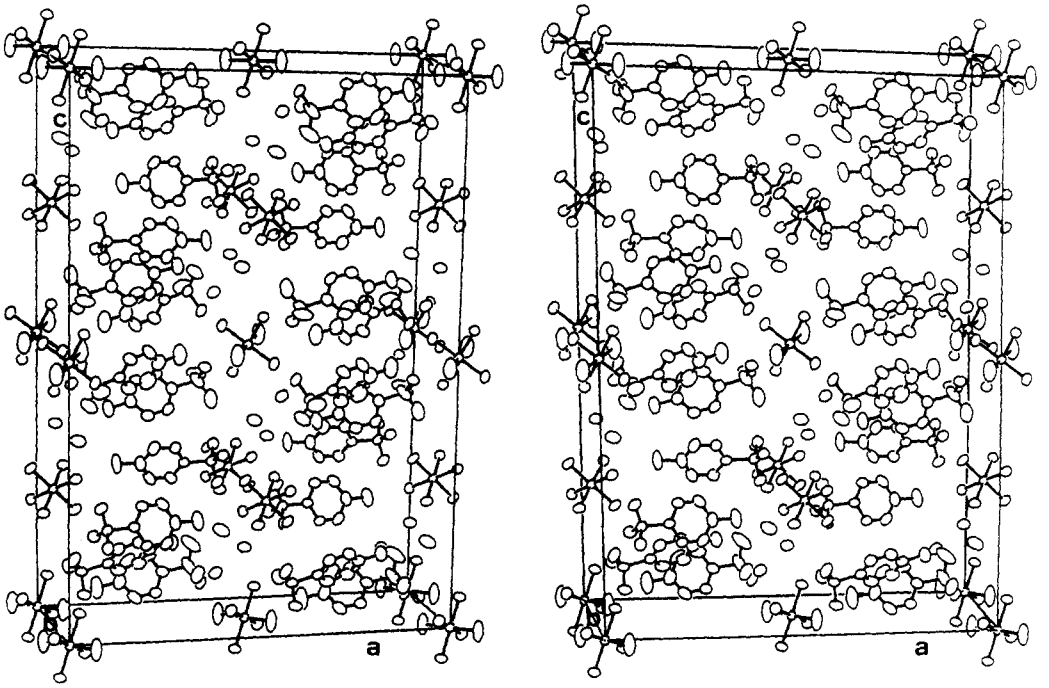

Figure 2. Stereoscopic view of the unit cell of $Ru(H_2O)_6(tos)_3 \cdot 3H_2O$ (III). Only the nonstarred atoms are plotted (Table IV).

ligand distances in the structures of pentaammine(pyrazine)ruthenium complexes.[14]

Rigid-body analyses[15] were done for the ruthenium hexaaqua ions in both oxidation states with the program THMI.[16] For the $Ru(H_2O)_6^{2+}$ and the ordered $Ru(H_2O)_6^{3+}$ the R values $[\sum(U_{ij}(\text{calcd}) - U_{ij}(\text{obsd}))^2/\sum(U_{ij}(\text{obsd}))^2]^{1/2}$ were 0.054 and 0.044 for 24 and 22 observations, respectively. Coordinates of the new oxygen positions were calculated. All corrections in bond lengths appeared to be less than 0.01 Å, the mean bond length being shifted from 2.122 to 2.130 Å for $Ru(H_2O)_6^{2+}$ and from 2.029 to 2.038 Å for $Ru(H_2O)_6^{3+}$. Neglect of this correction introduces a bias into the Ru–O distances, which is probably the same in order of magnitude as but opposite in sign to the bias due to the neglect of the water hydrogen atoms, which were not found in a difference Fourier synthesis and therefore not included in the structure factor calculations. In any case, the difference between the Ru–O distances in the two oxidation states is not appreciably affected.

The Ru1 ion at (0, 0, 0) shows two orientations of the coordination octahedron with oxyygen atoms O2, O3 and O2*, O3*, respectively. The oxygen atom O1 is not split but shows large vibrational parameters perpendicular to the direction of the Ru1–O1 bond (Figure 3). Consequently, this bond is shorter than all other Ru–O distances, and the bond angles involving O1 show large deviations from 90° (~7°, Table VII). For an interpretation of the apparent thermal motion of O1, eigenvalues and eigenvectors of the U tensor were calculated. The eigenvectors belonging to the two large eigenvalues are approximately perpendicular to the Ru1–O1 bond (88, 82°). The thermal motion correction, $\Delta = [U_1(O1) + U_2(O1) - U_1(Ru1) - U_2(Ru1)]/2d(Ru1-O1)$, for the Ru1–O1 bond length is ~0.048 Å.[17] The corrected bond

(14) Gress, M. E.; Creutz, C.; Quicksall, C. O. *Inorg. Chem.* **1981**, *20*, 1522.
(15) Schomaker, V.; Trueblood, K. N. *Acta Crystallogr., Sect. B* **1968**, *B24*, 63.
(16) We thank Professor K. Trueblood, UCLA, for a copy of his program.
(17) Busing, W. R.; Levy, H. A. *Acta Crystallogr.* **1964**, *17*, 142.

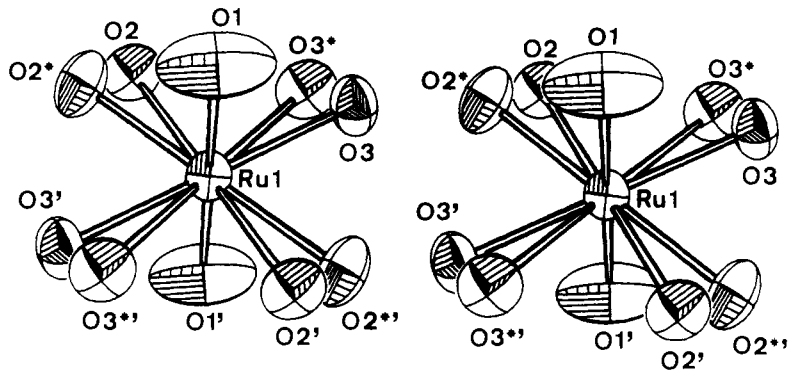

Figure 3. Stereoscopic view of the disordered $Ru(H_2O)_6^{3+}$ octahedron (Ru1) in the structure of III.

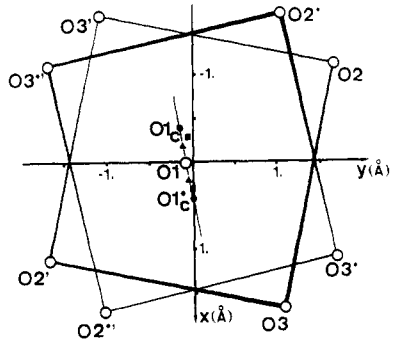

Figure 4. Projection of the disordered $Ru(H_2O)_6^{3+}$ octahedron (Ru1) onto the best plane of Ru1, O2, O2*, O3, O3*. The symbols ●, ■, and ▲ are explained in the text.

length is ~2.06 Å, rather long compared to the bond lengths not affected by large apparent thermal motion. Using the correction in bond length, we have estimated alternative positions displaced by 0.41 Å from O1 along either direction of the eigenvector belonging to the largest eigenvalue (● in Figure 4).[18] The resulting Ru1–O1 bonds are within 2.9° of the vector normal to the plane Ru1, O2, O3 (Ru1, O2*, O3*; ■ in Figure 4). Using half the correction to the mean position of O1 (▲ in Figure 4; $O1_c$, $O1_c$* used in all subsequent discussion) leads to Ru1–$O1_c$ (Ru1–$O1_c$*) distances of 2.026 Å, in accord with the average of the other Ru–O distances (2.029 Å, Table VII). The corresponding bond angles are close to 90°.

The disorder observed around Ru1 is related to a corresponding disorder in O23, O23* and O33, O33* bonded to S2 and S3, respectively, as well as to a disorder in the water molecule O9, O9* (Figure 5). Furthermore S2, O21, O22, S3, O31, and O32 show large apparent thermal motion. A network of chemically acceptable hydrogen bonds (>2.5 Å) may be traced as follows. Consider rows of Ru1 along *b*, specifically Ru1 at (0, 0, 0) with unstarred oxygen atoms $O1_c$, O2, O3, and Ru1 at (0, 1, 0) with starred oxygen atoms $O1_c$*, O2*, O3*. Choose among O23, O23*, O33, and O33* such that the resulting O···O distances are longer than 2.5 Å. The result is a hydrogen-bond network with periodicity 2*b* and inversion centers at (0, 0, 0) and (0, 1, 0) but not at (0, $^1/_2$, 0) (Figure 5). Note that rows of Ru1 are separated by rows of Ru2 (at 0, 0.4746, 0.25; Figure 2) and that oxygen atoms associated directly (O4–O6) or indirectly (O7–O8) with Ru2 make equally good hydrogen bonds to the starred and unstarred atoms; as a consequence the hydrogen-bond networks in neighboring rows of Ru1 are virtually uncorrelated and the structure does not show doubling of *b* but appears disordered.

(18) The displacement is consistent with the corrected bond length of 2.06 Å.

The average Ru–O bond length of $Ru(H_2O)_6^{2+}$ not corrected for effects of thermal motion is 2.122 (16) Å, significantly longer than the analogous mean Ru–O distance of 2.029 (7) Å in $Ru(H_2O)_6^{3+}$ where the distance Ru–O1 was not included in the average because of disorder (cf. preceding section). This change in bond length of 0.09 (2) Å on going from one oxidation state to the other is considerably larger than the variations within the coordination units of either II and III. Analogous structural comparisons may be made with ruthenium ammine complexes for which a few crystal structures have been determined.[19] For the parent complexes $Ru(NH_3)_6^{3+}$ and $Ru(NH_3)_6^{2+}$ cubic site symmetry imposes six equal Ru–N distances. The difference in Ru–N bond lengths is 0.040 (6) Å.[20] Thus a change in oxidation state has a significantly larger effect on Ru–O than on Ru–N lengths. This observation has been discussed qualitatively in terms of a π interaction that was said to be possible for H_2O but not for NH_3.[8] Since no precise information is available about the electronic structure of these complexes, we are not in a position to offer a more detailed interpretation.

In the remainder we discuss the relation between the salient structural result, namely, the bond length changes of 0.09 (2) and 0.04 (1) Å for the $Ru(H_2O)_6^{3+/2+}$ and $Ru(NH_3)_6^{3+/2+}$ couples on the one hand and chemical reactivity on the other.

Structural differences of the type described above have been shown to manifest themselves in the rates of electron-transfer reactions (self-exchange), e.g.

$$ML_6^{2+} + ML_6^{3+} \overset{k}{\rightleftharpoons} ML_6^{3+} + ML_6^{2+} \qquad (1)$$

For the pairs $Fe(H_2O)_6^{3+/2+}$, $Ru(H_2O)_6^{3+/2+}$, and $Ru(NH_3)_6^{3+/2+}$ rate constants k_{obsd} of 4.2, 6.0 × 10, and 4.3 × 10^3 s^{-1} M^{-1} have been observed or estimated.

The dependence of the rate constant k on various parameters has been modeled on the Marcus theory[4] as shown by eq 2–5.

$$k = (kT/h)\exp(-\Delta G^*/RT) \qquad (2)$$

$$\Delta G^* = w + \Delta G^*_{tr} + \Delta G^*_{out} + \Delta G^*_{in} \qquad (3)$$

$$\Delta G^*_{out} = \frac{e^2}{4}\left(\frac{1}{2a_{II}} + \frac{1}{2a_{III}} - \frac{1}{d}\right)\left(\frac{1}{n^2} - \frac{1}{D}\right) \qquad (4)$$

$$\Delta G^*_{in} = \frac{3f_{II}f_{III}(\Delta r)^2}{f_{II} + f_{III}} = 3\bar{f}(\Delta r)^2/2 \qquad (5)$$

In these expressions w is the work for bringing the two reactants together, ΔG^*_{tr} is the energy to form the transition state from two noninteracting complexes tumbling independently.

(19) For complexes of the type $Ru(NH_3)_5L^{3+/2+}$ and $Ru(NH_3)_4L_2^{3+/2+}$ Ru(II)–NH_3 distances vary between 2.02 and 2.199 Å and Ru(III)–NH_3 distances between 2.104 and 2.18 Å.[14] Clearly, electronic effects owing to the π acid L are a dominant factor here and may overrule the influence of the change in oxidation state.

(20) Stynes, H. C.; Ibers, J. A. *Inorg. Chem.* **1971**, *10*, 2304.

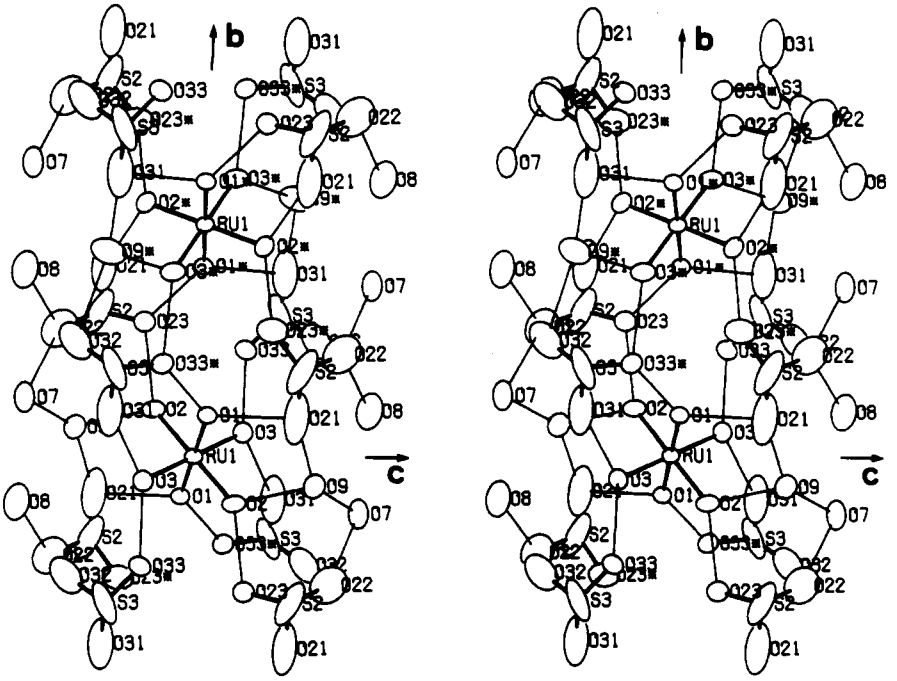

Figure 5. Stereoscopic view of the hydrogen bonds involving the disordered $Ru(H_2O)_6^{3+}$ (Ru1) in the structure of III.

$\Delta G^{\ddagger}_{out}$ and $\Delta G^{\ddagger}_{in}$ represent the energies of reorganization necessary to reach a transition-state structure for the outer and inner coordination shells, respectively. The quantities a_{II}, a_{III} and f_{II}, f_{III} are the radii and breathing force constants, respectively, of the two reactants; d is the distance between the metal atoms in the activated complex; for realistic values of f_{II} and f_{III} the reduced force constant $\bar{f}$[21] may be approximated by the (geometric or arithmetic) mean of f_{II} and f_{III}; n and D are the refractive index and the dielectric constant of the solvent, and Δr is the difference of the metal–ligand distances between the oxidized and reduced complex.

Estimates of the sum of w, $\Delta G^{\ddagger}_{tr}$, and $\Delta G^{\ddagger}_{out}$ have been given as 10.1 kcal mol^{-1} for $Fe(H_2O)_6^{3+/2+}$ and 10.9 kcal M^{-1} for $Ru(NH_3)_6^{3+/2+}$. We adopt the latter value also for $Ru(H_2O)_6^{3+/2+}$. Differences in activation energy >1 kcal mol^{-1} would therefore have to arise from the term $\Delta G^{\ddagger}_{in} = 3\bar{f}(\Delta r)^2/2$. Reasonable values for $\bar{f}$ are in the range 2–3 mdyn Å^{-1}; we adopt 2.5 (5) mdyn Å^{-1}. The values of Δr are 0.14 (2), 0.09 (2), and 0.04 (1) Å for $Fe(H_2O)_6^{3+/2+}$, $Ru(H_2O)_6^{3+/2+}$, and $Ru(NH_3)_6^{3+/2+}$, respectively, leading to $\Delta G^{\ddagger}_{in}$ = 10.5 (3.7), 4.4 (2.1), and 0.9 (0.5) kcal mol^{-1} and calculated logarithmic rate constants log k_{calcd} = −2.4 (2.7), 1.6 (1.6), and 4.2 (0.3). These numbers compare well with observed values log k_{obsd} = 0.6, 1.8, and 3.6, respectively. It should be noted, however, that the uncertainties in $\bar{f}$ and especially in the squared term $(\Delta r)^2$ affect the calculated rate constants quite dramatically, in particular for $Fe(H_2O)_6^{3+/2+}$. Improved estimates of Δr are difficult to obtain since the uncertainty in Δr is due more to intrinsic differences among individual bond lengths than to inaccuracy in the determination. These differences reflect the differences in the solid-state environment, and analogous differences have to be taken into account in solution. Similar arguments apply also to the force constants.

In summary, we conclude that the observed order of rate constants $k[Fe(H_2O)_6^{3+/2+}] < k[Ru(H_2O)_6^{3+/2+}] < k[Ru(NH_3)_6^{3+/2+}]$ may be rationalized in a qualitative way in terms of the reorganization energies $\Delta G^{\ddagger}_{in}$ during self-exchange. These energies as estimated from the difference in metal to ligand distance decrease in the order $\Delta G^{\ddagger}_{in}[Fe(H_2O)_6^{3+/2+}] > \Delta G^{\ddagger}_{in}[Ru(H_2O)_6^{3+/2+}] > \Delta G^{\ddagger}_{in}[Ru(NH_3)_6^{3+/2+}]$.

The new results fit quite nicely within the general frame of the Marcus theory for outer-sphere electron-transfer reactions. Work is in progress in our laboratory to determine the stretching vibrations of II and III as a further step toward the understanding of the self-exchange reaction of the $Ru(H_2O)_6^{3+/2+}$ couple. An independent and direct measurement of this electron-transfer rate would be a very important and valuable piece of information.

Acknowledgment. We thank Dr. H. Wagner, Ciba-Geigy AG, for the elemental analyses and one of the reviewers for his suggestions concerning the discussion of the hydrogen bond network. This work was supported by the Swiss National Science Foundation.

Registry No. II, 15694-44-7; III, 82903-51-3; $Ru(H_2O)_6^{3+}$, 30251-72-0; $Ru(H_2O)_6^{2+}$, 30251-71-9.

Supplementary Material Available: Listings of structure factors, thermal parameters, hydrogen positions, least-squares planes of the anions, and bond lengths and angles of the anions for II and III (43 pages). Ordering information is given on any current masthead page.

(21) Brunschwig, B. S.; Logan, J.; Newton, M. D.; Sutin, N. *J. Am. Chem. Soc.* **1980**, *102*, 5798.